Available online at www.sciencedirect.com

SCIENCE DIRECT

Biochimica et Biophysica Acta 1709 (2005) 84 – 94

BIOCHIMICA ET BIOPHYSICA ACTA
BBA

http://www.elsevier.com/locate/bba

Role of transmembrane segment 5 of the plant vacuolar H^+-pyrophosphatase

Ru C. Van, Yih J. Pan, Shen H. Hsu, Yun T. Huang, Yi Y. Hsiao, Rong L. Pan*

Department of Life Sciences and Institute of Bioinformatics and Structural Biology, College of Life Sciences, National Tsing Hua University, Hsin Chu 30043, Taiwan, Republic of China

Received 8 April 2005; received in revised form 26 May 2005; accepted 31 May 2005
Available online 20 June 2005

Abstract

Vacuolar H^+-translocating inorganic pyrophosphatase (V-PPase; EC 3.6.1.1) is a homodimeric proton translocase consisting of a single type of polypeptide with a molecular mass of approximately 81 kDa. Topological analysis tentatively predicts that mung bean V-PPase contains 14 transmembrane domains. Alignment analysis of V-PPase demonstrated that the transmembrane domain 5 (TM5) of the enzyme is highly conserved in plants and located at the N-terminal side of the putative substrate-binding loop. The hydropathic analysis of V-PPase showed a relatively lower degree of hydrophobicity in the TM5 region as compared to other domains. Accordingly, it appears that TM5 is probably involved in the proton translocation of V-PPase. In this study, we used site-directed mutagenesis to examine the functional role of amino acid residues in TM5 of V-PPase. A series of mutants singly replaced by alanine residues along TM5 were constructed and over-expressed in *Saccharomyces cerevisiae*; they were then used to determine their enzymatic activities and proton translocations. Our results indicate that several mutants displayed minor variations in enzymatic properties, while others including those mutated at E225, a GYG motif (residues from 229 to 231), A238, and R242, showed a serious decline in enzymatic activity, proton translocation, and coupling efficiency of V-PPase. Moreover, the mutation at Y230 relieved several cation effects on the V-PPase. The GYG motif presumably plays a significant role in maintaining structure and function of V-PPase.

Keywords: Proton translocation; Tonoplast; Vacuole; Vacuolar H^+-pyrophosphatase; Site-directed mutagenesis; GYG motif

1. Introduction

The H^+-translocating vacuolar pyrophosphatase (V-PPase, EC 3.6.1.1) is an integral protein that utilizes solely PP_i as the substrate to generate an inside-acidic and inside-positive electrochemical potential for many secondary transports of ions and metabolites across the vacuolar membranes [1,2]. The V-PPase contains a distinct kind of polypeptide with a molecular mass of approximately 81 kDa, which presumably forms a homodimer as determined by gel filtration and radiation inactivation analysis [1,3]. However, a single catalytic subunit of the dimeric V-PPase is sufficient for displaying the hydrolytic activity of the enzyme but insufficient for performing its H^+-translocating reaction [1,3]. Vacuolar H^+-PPase requires Mg^{2+} as a cofactor and the binding of Mg^{2+} stabilizes and activates the enzyme [1,4]. Relatively high concentration of K^+ could stimulate vacuolar H^+-PPase, while excess PP_i, Ca^{2+}, Na^+, and F^- inhibit its enzymatic activity [5–7]. Furthermore, the biochemical and phylogenetic analyses demonstrated the existence of isoforms with respect to K^+-requirement [8,9]. Nevertheless, it is conceivable that the vacuolar H^+-PPase accommodates binding domains for the substrate and the above-mentioned ligands, as well as proton translocation.

The hydropathic analysis predicted that the single polypeptide of V-PPase consists of 14–16 α-helical transmembrane domains [1,10]. Lines of evidence demonstrate that the catalytic pocket of V-PPase, facing cytosolic side, is probably composed of 2–3 conserved segments (cf., [1]). A fragment of DX_7KXE on cytosolic loop 3 (CL3) was suggested as the

Abbreviations: CL, cytosolic loop; DTT, dithiothreitol; EGTA, ethyleneglycol-bis-(β-amino-ethylether) *N,N,N′,N′*-tetraacetic acid; PMSF, phenylmethylsulfonyl fluoride; TM, transmembrane segment; V-PPase, vacuolar H^+-pyrophosphatase

* Corresponding author. Tel./fax: +886 3 5742688.
E-mail address: rlpan@life.nthu.edu.tw (R.L. Pan).

0005-2728/$ - see front matter © 2005 Published by Elsevier B.V.
doi:10.1016/j.bbabio.2005.05.011

putative substrate-binding region by an immunochemical study with an antibody specific to this sequence [11]. A *N*-ethylmaleimide-binding cysteine residue (Cys-634) and numerous *N*,*N*′-dicyclohexylcarbodiimide-binding residues (Glu-305 and Asp-283 on CL3 and Asp-504 on CL5) have been identified by the combination of site-directed mutagenesis and chemical modification as essential residues involved in enzymatic and proton-translocating reactions of V-PPase [12–14]. Furthermore, several functional charged residues and two acidic fragments of DX_3DX_3D on either CL3 or CL7 were implicated as crucial residues in substrate-binding domains [15]. It is also proposed that the catalytic domains of V-PPase include not only the substrate-binding motif but also the binding sites for cations, such as Mg^{2+} and K^+ [15]. In addition, phylogenetic analysis along with site-directed mutagenesis revealed possible involvement in K^+ binding at A460 of the H^+-PPase from *C. hydrogenoformans* [8]. Substitution of A460 by lysine residue could convert H^+-PPase of *C. hydrogenoformans* from K^+-sensitive to K^+-insensitive forms [8]. All these essential sites for the enzymatic activation were localized in the cytosolic loop regions of V-PPase. Nevertheless, no consensus on the domains involved in proton translocation of V-PPase has been successfully drawn.

Topological analysis on the TopPred II program [16] tentatively predicts that mung bean V-PPase contains 14 transmembrane domains (Fig. 1). Alignment analysis of V-PPase demonstrates that the transmembrane domain 5 (TM5), residues from 221 to 242, of the enzyme is highly conserved in plants (Fig. 1C) and located at the N-terminal side of the CL3 loop that presumably contains highly conserved sequences and a putative substrate-binding motif. Furthermore, the hydropathic analysis of V-PPase showed a relatively lower degree of hydrophobicity in TM5 region than other domains. Accordingly, we speculate that TM5 is probably involved in the proton translocation of V-PPase. In this study, we used the site-directed mutagenesis to examine the functional role of amino acid residues in TM5 of V-PPase. A series of mutants singly replaced by alanine residues along TM5 were constructed, over-expressed in *Saccharomyces cerevisiae*, and then used to determine their enzymatic activities and proton translocations. Our results indicate that several mutants displayed minor variations in enzymatic properties, while others including those mutated at E225, a GYG motif (residues from 229 to 231), A238, and R242, showed a serious decline in enzymatic activity, proton translocation, and coupling efficiency of V-PPase. Moreover, the mutation at Y230 also relieved the cation

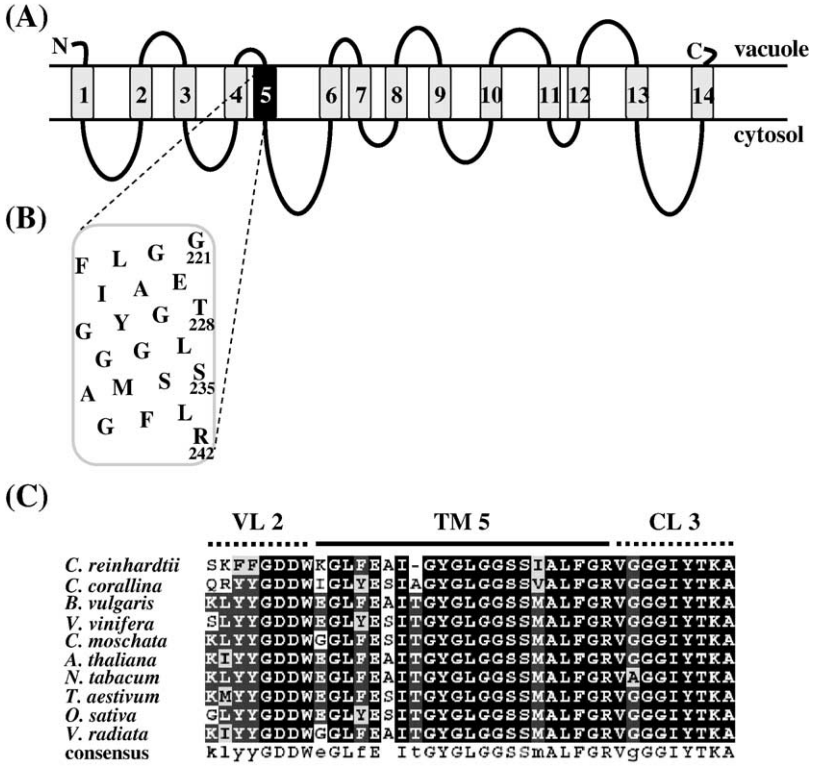

Fig. 1. TM5 of plant V-PPases. (A) Topological model of plant V-PPase. The model of plant V-PPase containing 14 transmembrane domains is proposed using TopPred II program [16]. (B) Amino acid sequence of TM5 α-helix. (C) Alignment of TM5 segments from various V-PPases. Amino acid sequences of TM5 from a set of plant V-PPases were aligned using the Pileup program of the University of Wisconsin Genetics Computer Group (GCG). The GenBank accession numbers for V-PPases of each species are: *Chlamydomonas reinhardtii*, CAC44451; *Chara corallina*, BAA36841; *Beta vulgaris*, AAA61609; *Vitis vinifera*, AAF69010; *Cucurbita moschata*, BAA33149; *Arabidopsis thaliana*, A38230; *Nicotiana tabacum*, S61423; *Triticum aestivum*, AAP55210; *Oryza sativa*, BAA08232; *Vigna radiata*, P21616.

effects on the V-PPase. The GYG motif presumably plays a significant role in maintaining structure and function of V-PPase.

2. Materials and methods

2.1. Microorganisms

The *E. coli* strain XL1-blue (*rec*A1, *end*A1, *gyr*A96, *thi-1*, *hsd*R17(r_k^-,m_k^+), *sup*E44, *rel*A1, *lac* [F′ *pro*AB, *lac*I^{q}ZΔ*M15*, Tn10 (Tet^r)]) was used for manipulation of plasmids and the vacuolar protease-deficient *Saccharomyces cerevisiae* strain BJ2168 (*MATa*, *prc1-407*, *prb1-1122*, *pep4-3*, *leu2*, *trp1*, *ura3-52*) for heterologous expression of V-PPase. The mutated V-PPase cDNA was finally constructed into a vector pYES2 (Invitrogen, Carlsbad, CA, USA) after *GAL1* promoter between *Hind*III and *Xba*I, for expression. Yeast was transformed according to the method of Gietz et al. [17] and grown in YPG medium [1% (w/v) yeast extract (DIFCO, Detroit, MI, USA), 2% (w/v) bactopeptone (DIFCO, Detroit, MI, USA), and 2% (w/v) galactose].

2.2. Site-directed mutagenesis

Mutagenic oligonucleotides were designed to generate each single alanine substitution along TM5 of mung bean V-PPase by PCR megaprimer method using *Vent*® as the DNA polymerase [18]. However, the original alanine codons in TM5 were changed to serine, respectively. The sequences of the mutated oligonucleotides were shown as below and confirmed by DNA autosequencing (codons of mutated residues were presented in brackets and positions of changed nucleotide underlined):

G221A, 5′-GATGACTGG[GCT]GGTCTTTTTG-3′;
G222A, 5′-TGGGGT[GCT]CTTTTTGAG-3′;
L223A, 5′-GGTGGT[GCT]TTTGAGGCC-3′;
F224A, 5′-GGTCTT[GCT]GAGGCCATA-3′;
E225A, 5′-CTTTTT[GCG]GCCATAACT-3′;
A226S, 5′-GGTCTTTTTGAG[TCC]ATAACTGG-3′;
I227A, 5′-GAGGCC[GCA]ACTGGTTAT-3′;
T228A, 5′-GCCATA[GCT]GGTTATGGT-3′;
G229A, 5′-ATAACT[GCT]TATGGTCTC-3′;
Y230A, 5′-ACTGGT[GCT]GGTCTCGGT-3′;
G231A, 5′-GGTTAT[GCT]CTCGGTGGG-3′;
L232A, 5′-TATGGT[GCC]GGTGGGTCT-3′;
G233A, 5′-GGTCTC[GCT]GGGTCTTCT-3′;
G234A, 5′-CTCGGT[GCG]TCTTCTATG-3′;
S235A, 5′-GGTGGG[GCT]TCTATGGCT-3′;
S236A, 5′-GGGTCT[GCT]ATGGCTTTG-3′;
M237A, 5′-TCTTCT[GCG]GCTTTGTTC-3′.
A238S, 5′-TCTATG[TCT]TTGTTCGGA-3′;
L239A, 5′-ATGGCT[GCG]TTCGGAAGA-3′;
F240A, 5′-GCTTTG[GCC]GGAAGAGTT-3′;
G241A, 5′-TTGTTC[GCA]AGAGTTGGC-3′;
R242A, 5′-TTCGGA[GCA]GTTGGCGGA-3′.

The final PCR products were digested with appropriate restriction enzymes and inserted to pYES2 for heterologous expression in yeast [19].

2.3. Preparation of yeast microsomes

Yeast microsomes were prepared according to Kim et al. with minor modifications [12,19]. The yeast cell culture was grown at 30 °C for 3 days in the CM medium [0.5% (w/v) ammonium sulfate, 2% (w/v) galactose, 0.2% (w/v) yeast nitrogen base without amino acids and ammonium sulfate, 60 μg/mL leucine, and 40 μg/mL tryptophan]. The cells were collected by centrifugation at 4,000×*g* at 4 °C for 10 min and resuspended in a washing medium [100 mM Tris–HCl (pH 9.4) and 10 mM DTT]. After gentle shaking at 37 °C for 20 min, the cells were pelleted as above and then resuspended in the YP lysis medium [100 mM Tris–Mes (pH 8.0), 1% (w/v) yeast extract, 2% (w/v) peptone, 0.7 M sorbitol, 1% (w/v) glucose, and 5 mM DTT]. Following lyticase digestion (150 μg/mL) with gentle shaking at 30 °C for 90 min, the cells were pelleted as above, and resuspended in the ice-cold homogenization medium [10% (w/v) glycerol, 1.5% (w/v) PVP, 5 mM Tris–EGTA, 2 mg/mL BSA, 50 mM Tris–ascorbate (pH 7.6), 1 mM PMSF, and 1 μg/mL pepstatin A]. The suspension of spheroplasts was homogenized in a Dounce homogenizer, followed by differential centrifugation at 4,000×*g* for 10 min and 75,000×*g* for 35 min at 4 °C. The pellet was resuspended in a suspension medium [10.25% (w/v) glycerol, 2 mM DTT, 1 mM Tris–EGTA, 5 mM Tris–Mes (pH 7.5), 2 mg/mL BSA, 2 mM DTT, 1 mM PMSF, and 1 μg/mL pepstatin A], layered onto a discontinuous 10%/28% (w/v) sucrose density gradient in the suspension medium, and centrifuged at 75,000×*g* at 4 °C for 2 h. The partially purified yeast microsomes containing the vacuolar H^+-PPase were withdrawn from the 10%/28% (w/v) interface, diluted 9-fold with storage buffer [10% (w/v) glycerol and 5 mM Tris–Mes (pH 7.5)], and then pelleted by centrifugation at 75,000×*g* at 4 °C for 55 min. The yeast microsomes were finally resuspended in the storage buffer and stored at −70 °C for further use.

2.4. Measurements of enzymatic activities and protein concentration

The enzymatic activity of vacuolar H^+-PPase was measured as the rate of P_i released from PP_i [20]. Yeast microsomes were incubated at 37 °C in the reaction medium [30 mM Tris–Mes (pH 8.0), 1 mM $MgSO_4$, 50 mM KCl, 0.5 mM NaF, 1 mM Na_4PP_i, 1.5 μg/mL gramicidin D, and 20 μg/mL microsome proteins]. The reaction was then terminated by a stop-solution [0.7% (w/v) ammonium molybdate, 2.0% (w/v) sodium dodecyl sulfate, 0.02% (w/v) 1-amino-2-naphthol-4-sulphonic acid, and 1.16 N HCl] and the released P_i measured spectrophotometrically as described elsewhere [20,21]. For heat treatment, yeast

microsomes were pre-incubated at temperature indicated for 10 min and then put on ice bath immediately, followed by activity assays as described above. To determine ion effects, 100 mM NaCl, 0.1 mM $CaCl_2$, and 10 mM KF were added, respectively, into reaction solutions, if present. For determination of optimal pH, different pH values of reaction media were maintained in Tris–Mes buffer. Lineweaver–Burk plots were obtained conventionally and values of K_M and V_{max} were thus yielded using the Sigmaplot 5.0 software (SPSS, Chicago, IL, USA).

Protein concentration was calculated according to the Bradford method with BSA as a standard [22].

2.5. Measurement of the PP_i-dependent proton translocation

The PP_i-dependent H^+ translocation was traced by measuring the fluorescence quenching of acridine orange (Sigma, St. Louis, MO, USA) using excitation wavelength at 490 nm and emission wavelength at 530 nm [19,23–25]. Yeast microsomes (50 μg/mL) were added into the assay medium [100 mM KCl, 400 mM glycerol, 1 mM Tris–EGTA, 5 mM Tris–HCl (pH 8.0), 1.3 mM $MgSO_4$, and 5 μM acridine orange]. After equilibration, the reaction was initiated by adding 1 mM Na_4PP_i. The initial rate of fluorescence quenching was calculated as the proton transport activity [19,23–25]. The ionophore, gramicidin D (3 μg/mL), was included at the end of each assay to confirm the integrity of the membrane. Apparent coupling ratio (the ratio of initial proton pumping rate to that of PP_i hydrolysis) was measured as ($\Delta F\%$ min^{-1})/(μmol PP_i hydrolyzed min^{-1}) according to Zhen et al. [13].

2.6. SDS-PAGE and Western analysis

The samples were delipidated in 50 volumes of chloroform/methanol mixture (1:1, v/v) at −20 °C for 3–4 h and then subjected to SDS-PAGE according to Laemmli [26]. The gels were stained with silver stain or electrotransferred to PVDF membrane by using the semi-dry electrotransblotting apparatus (Nova Blot, Amersham Pharmacia Biotech, Piscataway, NJ, USA). The blots were incubated with the rabbit polyclonal antibody raised against the MAP-conjugated synthetic peptide of the sequence KVERNIPEDDPRNPA, which corresponds to positions from 261 to 275 of substrate-binding domain of mung bean vacuolar H^+-PPase. Bands of immunoblots were visualized using the chemiluminescence kit (New England Nuclear, Boston, MA, USA) as the manufacturer recommended.

2.7. Control over K^+, Na^+, and Ca^{2+} contamination

The background concentrations of K^+, Na^+, and Ca^{2+} in our assay media were below 4.0, 5.0, and 20 nM, respectively, as determined by ICP-AES (Inductively coupled plasma-atomic emission spectrometer) at NTHU Instrument Center, National Tsing Hua University, Hsin Chu, Taiwan.

2.8. Chemicals

Restriction endonuclease and T_4 DNA ligase were purchased from New England Biolabs (Beverly, MA, USA). Immunoblotting reagents were obtained from Bio-Rad (Hercules, CA, USA) and PP_i from E. Merck (Damstadt, Germany). All other chemicals were of analytic grade and used without further purification.

3. Results

3.1. Expression and enzymatic activity of mung bean V-PPase in yeast

A yeast expression vector pYES2 was used to express mung bean vacuolar H^+-PPase encoding cDNA (VVP) and the H^+-PPase was transcribed efficiently by transformant under the control of the *GAL1* promoter (cf., [19]). The V-PPase-enriched membranes from yeasts were successfully prepared by a sucrose gradient centrifugation and subsequent immunoblotting analyses revealed that a 73-kDa protein could be solely recognized by antibodies with polyclonal antibodies specific to deduced substrate-binding site of V-PPase (Fig. 2A). Total membrane proteins of routinely isolated microsomal vesicles consisted of expressed V-PPase at approximately 10–15% level (data not shown). Furthermore, the partially purified microsomal membranes of the transformant with pYES2 alone showed negligible PPase activity. However, the microsomal membranes of transformant with pYES2-VVP displayed PP_i hydrolytic and PP_i-mediated proton translocating activities (Fig. 2B and C). Both reactions of the transformant were significantly stimulated by 50 mM KCl, but substantially inhibited by 100 mM NaCl, 0.1 mM $CaCl_2$, and 10 mM KF, respectively (Fig. 2B and C). Moreover, the PP_i-dependent pH gradient could be collapsed by the addition of ionophore, gramicidin D, indicating membrane integrity and the electrogenic H^+-transport in vesicles. These results concur consistently with the general properties of mung bean vacuolar H^+-PPase, suggesting our expression system is proper for following studies.

3.2. Enzymatic activities and the proton translocation of TM5 mutants

To investigate the role of V-PPase TM5, this segment was subjected to alanine-scanning mutagenesis. A single substitution of each residue along TM5 by alanine was performed, except that original alanine residues at positions 226 and 238 were replaced by serine, respectively. The variants individually mutated at residues along TM5 could express V-PPase with appropriate efficiency as

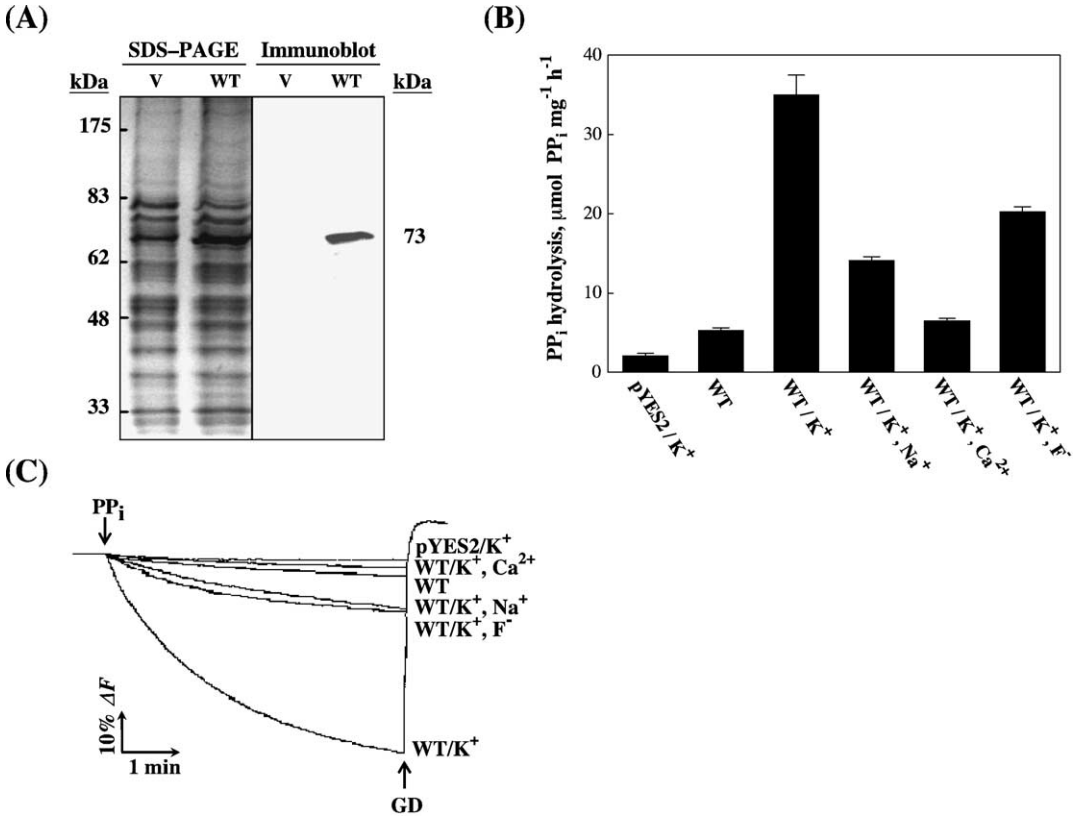

Fig. 2. Heterologous expression of mung bean V-PPase in yeast. (A) The expression of V-PPase in yeast. Both constructs accommodating wild type V-PPase (WT) or vector alone (V) were transformed into and expressed in *S. cerevisiae*. Microsomal membrane fractions containing expressed V-PPase were prepared and then subjected to SDS-PAGE (left) and immunoblot analysis (right). Molecular masses (kDa) are indicated on both sides of the gels. (B) Enzymatic activities of V-PPase transformants. The measurements of enzymatic activities were as described under Materials and methods. The concentrations of ions were: 50 mM K^+, 100 mM Na^+, 0.1 mM Ca^{2+}, and 10 mM F^-, respectively. (C) PP_i-associated H^+ translocation. The reaction conditions for proton translocation were as described under Materials and methods. Proton transport was initiated by adding 1.0 mM PP_i. At end of each reaction, 3 μg/mL gramicidin D was added to stop the fluorescence quenching of acridine orange. GD, gramicidin D. Values are means ± S.D. from at least 3 separate experiments.

visualized by immunoblotting at positions in the vicinity of molecular mass of 73-kDa (Fig. 3A). PP_i hydrolytic and its associated proton translocating reactions of mutants were then scrutinized and shown in Fig. 3B and C. In general, most transformants retained relatively similar hydrolytic activities (ranging from ±30%) to the wild type except that enzymatic activities of E225A, G229A, and G231A were decreased to approximately half of wild type and those of Y230A and R242A were almost abolished. Mutations in the middle of the TM5 (G229 to G231) were more deleterious than other portion. These three residues (GYG motif) may presumably play a crucial role in sustaining the enzymatic reaction of vacuolar H^+-PPase. In addition, the charged residues in the border between membrane and cytosol (R242A) or within the transmembrane (E225A) are also decisive for the enzymatic activity. Furthermore, the initial proton pumping activities of mutants were examined and listed in Fig. 3C. Two major troughs, one at the GYG motif and the other at the segment from M237 to F240, in the profile of H^+-translocation were observed. The apparent coupling ratios for variants with mutation at residues in GYG motif were decreased seriously to less than 50% while other mutants still remained within 65% of the wild type (Fig. 3D), confirming as well the possible contribution of these three residues in proton transport. Meanwhile, these alterations came directly from the effect of single amino acid substitution, since all mutants displayed similar efficiency of expression in yeast microsomes.

3.3. Kinetics of V-PPase mutants

A conventional Lineweaver–Burk plot of vacuolar H^+-PPase yielded an apparent K_M value of 154 ± 4 μM and an apparent V_{max} value of 74.8 ± 2.1 μmol PP_i consumed mg protein^{-1} h^{-1} for substrate Mg^{2+}–PP_i, respectively (data not shown). The apparent K_M and V_{max} values of each mutant were then determined and are also summarized in Table 1. The changes in V_{max} value of mutants are coincident with the variation in their specific activities. Furthermore, eight mutants in TM5 region (E225A, G229A–G234A, and R242A) displayed lower V_{max} and K_M values than wild type, representing a decrease in the reactivity, but an increase in the accessibility of substrate to active site of

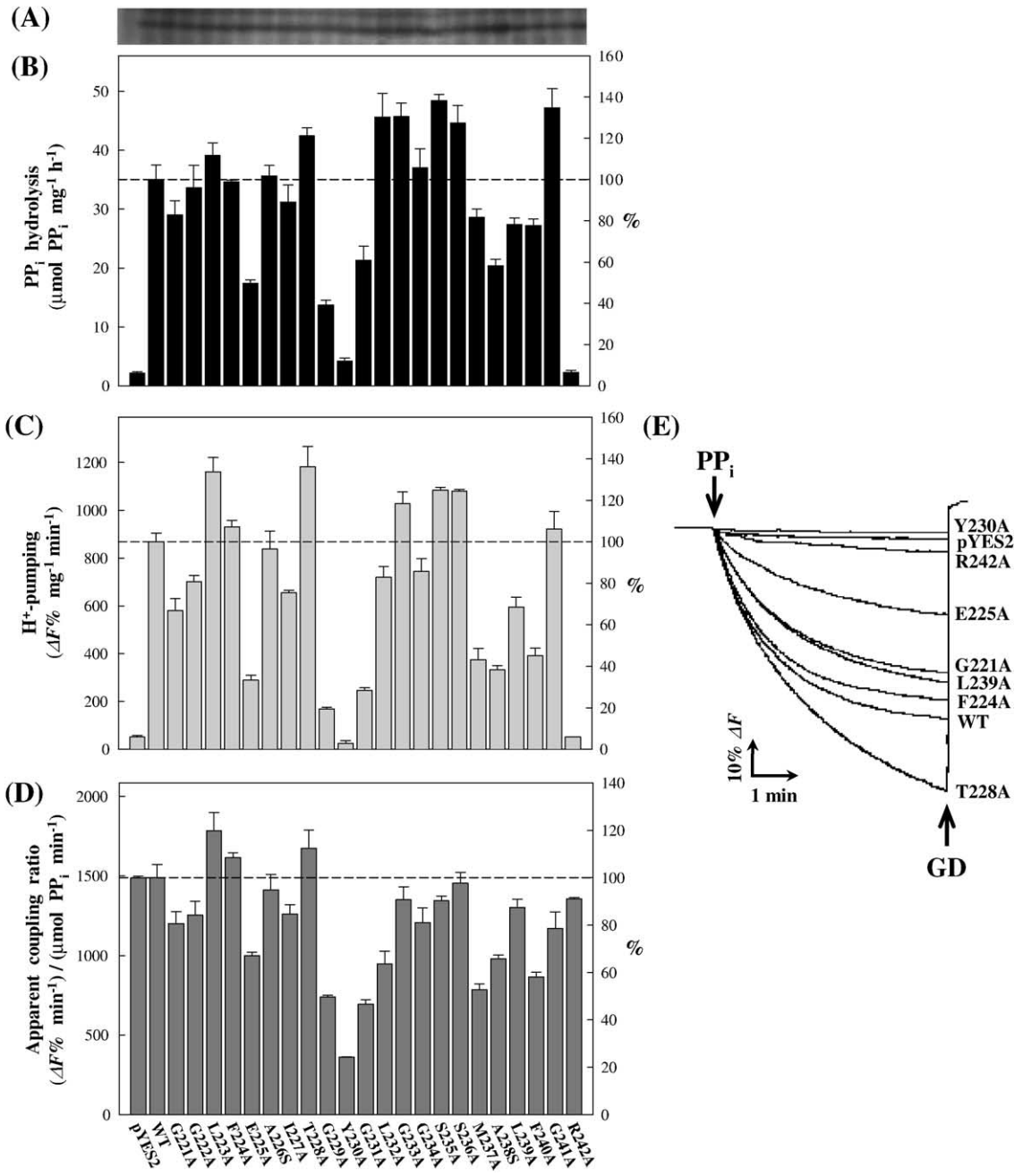

Fig. 3. Expression and reaction activities of mutant V-PPases. (A) Immunoblotting of V-PPase mutants. Microsomal membrane fractions were prepared from yeast transformed by wild type (WT) and mutant V-PPase DNAs, subjected to SDS-PAGE, and recognized by the anti-V-PPase antibody according the methods as described under Materials and methods. (B) PP_i hydrolysis activities of each mutant. (C) The PP_i dependent proton translocation of each mutant. (D) Relative coupling efficiency of each mutant. Apparent coupling ratio is expressed as ($\Delta F\%$ min^{-1})/(μmol PP_i hydrolyzed min^{-1}), where $\Delta F\%$ is the difference in relative fluorescence quenching of acridine orange. (E) Reaction trace of PP_i-dependent proton pumping. The measurements of enzymatic and proton translocating reactions were as described under Materials and methods. Values are means ± S.D. from at least 3 separate experiments.

V-PPase. In addition, four more mutants (G222A–F224A and G241A) gave relatively higher K_M and V_{max} values, showing a decrease in affinity of substrate to active sites of these mutants, but inversely an augmentation in their reactivity. We speculate that the mutation at these residues brought the conformation of the enzyme into different states, thus resulting in the changes of V_{max} and K_M values of these variants, respectively.

3.4. Ion effects and pH optima of V-PPase mutants

Ion effects on PP_i hydrolysis of V-PPase mutants were determined and summarized in Fig. 4. The enzymatic activity of wild type V-PPase in the absence of K^+ is 15% of that in the presence of 50 mM K^+; i.e., nearly 6.6-fold stimulation was observed (Fig. 4A). In contrast, the K^+-stimulation of enzymatic activity of Y230A was signifi-

Table 1
Kinetic properties of TM 5 mutants

Mutants	$T_{1/2}$ (°C)	pH optimum	K_M		V_{max}	
			μM	(%)	μmol PP_i mg^{-1} h^{-1}	(%)
Wild type	58.5	8.0	154±4	(100)	74.8±2.1	(100)
G221A	57.7	8.0	148±5	(96)	66.0±2.5	(88)
G222A	58.3	7.7	318±5	(207)	106.0±2.6	(142)
L223A	52.2	7.7	438±9	(284)	118.2±3.9	(158)
F224A	57.2	7.7	305±5	(198)	97.5±2.5	(130)
E225A	55.1	7.5	54±4	(35)	27.7±1.7	(37)
A226S	55.9	7.9	185±6	(120)	68.0±2.6	(91)
I227A	52.7	7.7	140±6	(91)	49.9±2.5	(67)
T228A	54.8	7.9	146±5	(95)	68.7±2.3	(92)
G229A	54.5	7.9	68±4	(44)	29.0±1.8	(39)
Y230A	54.5	7.4	8±1	(5)	4.3±0.3	(6)
G231A	59.4	7.6	16±2	(10)	23.8±0.7	(32)
L232A	52.6	8.0	35±2	(23)	54.1±1.0	(72)
G233A	58.7	8.1	74±4	(48)	62.1±1.8	(83)
G234A	58.9	7.8	70±5	(46)	51.4±2.2	(69)
S235A	55.4	7.9	199±5	(130)	88.1±2.3	(118)
S236A	54.3	7.7	105±6	(68)	65.6±2.7	(88)
M237A	57.7	8.1	112±5	(73)	46.9±2.3	(63)
A238S	54.4	7.8	196±7	(127)	58.3±2.9	(78)
L239A	51.0	7.5	221±9	(144)	71.9±3.9	(96)
F240A	49.8	7.5	99±6	(65)	44.1±2.7	(59)
G241A	56.6	7.9	332±12	(215)	127.3±5.3	(170)
R242A	54.6	7.4	22±1	(14)	7.6±0.5	(10)

Microsomes containing heterologously expressed V-PPase were prepared from *S. cerevisiae* and the measurements of enzymatic activities were as described under Materials and methods. For determination of optimal pH, different pH values of reaction media were maintained by adjusting pH value of Tris–Mes buffer. $T_{1/2}$ values were the pretreatment temperatures at which half enzymatic activity were observed. The K_M and V_{max} values were obtained directly from the conventional Lineweaver–Burk plots using the Sigmaplot 5.0 software. All values are means±S.D. from at least 3 separate experiments.

cantly decreased by 2/3 of wild type, while those of G231A, M237A, and R242A were by approximately 50%. The K^+-stimulation of the rest of mutants remained within 75% of wild type. The deleterious effect of mutation at Y230 on K^+-stimulation implies presumably its role in K^+-binding. Furthermore, the presence of Na^+, Ca^{2+}, and F^- inhibited the enzymatic activity of wild type V-PPase to approximately 40%, 19%, and 58% of control, respectively. Mutation of most residues along TM5, with exception at Y230 and R242, did not change the vulnerability of enzymatic activity to Na^+ inhibition. Besides, mutation at these two sites prevented the suppressing effect of Ca^{2+} on enzymatic activity of V-PPase. We suggest that these two residues probably participate in a general cation binding of V-PPase. Notwithstanding, they did not show any relief in F^- inhibition. The mechanism of F^- binding is likely distinct from that of other cations to V-PPase.

Fig. 5 depicts the pH profile of several variants mutated at residues along TM5 of vacuolar H^+-PPase. For the wild type, the optimal pH of vacuolar H^+-PPase is approximately at pH 8.0. Upon substitution of amino acid residues along TM5, optimal pH values of E225A, Y230A, L239A, F240A, and R242A were shifted to be more acidic by nearly 0.5 units. As for the rest of the variants, they were similar to wild type. The shift of optimal pH reveals probably that the enzyme conformation of these mutants is different from the wild type, consequently resulting in the exposure of other charged residues to the environments.

3.5. Thermal stability of V-PPase mutants

Vacuolar H^+-PPase was pretreated at different temperature and cooled on ice bath. The enzymatic activities of heat-treated vacuolar H^+-PPase were then measured and $T_{1/2}$ values (pretreatment temperature at which half enzymatic activity is then observed) determined (Fig. 6). The PP_i hydrolytic activity of wild type V-PPase was slightly increased as pretreatment temperature was raised to 45 °C, beyond which the activity declined progressively with the increase of temperature (Fig. 6A, -●-). The temperature profile displays a $T_{1/2}$ value of 58.5 °C for wild type V-PPase. Similarly, temperature profile and $T_{1/2}$ values of mutants were accordingly examined. Our results indicate, however, the $T_{1/2}$ values of most mutants were decreased as compared to wild type, with those of L223A, I227A, L232A, L239A, and F240A by more than 5 °C (Fig. 6B). Variants derived from mutation at amino acid residues with bulky side chains in TM5 were obviously more vulnerable to heat treatment.

4. Discussion

TM5 is a highly conserved transmembrane fragment locating at the N-terminal side of the putative substrate-binding loop of V-PPase. TM5 is customarily predicted as a α-helix fragment and shows a relatively lower degree of hydrophobicity than other transmembrane portions of V-PPase. This work reports the important roles of the amino acid residues along TM5 by alanine scanning mutagenesis method. Generally, the TM5 mutants could be divided into two groups with respect to deleterious effects on their specific activities. Group 1 includes mutants retaining relatively similar hydrolytic activities (ranging from ±30%) to the wild type. Group 2 consists of mutants with reduced specific activities (less than 50% of wild type): E225A, G229A, Y230A, G231A, A238S, and R242A.

Since Group 1 mutants possess similar hydrolytic activities of PP_i to wild type, majority of their enzyme features are preserved. However, there are still some minor variations in the enzyme properties of Group 1 mutants. For instance, although most Group 1 mutants showed similar proton translocating activities, M237A and F240A possessed lower apparent coupling ratios at approximately 50% of wild type. Furthermore, kinetic analysis indicates K_M values of some Group 1 mutants, such as G222A, L223A, F224A, and G241A, were increased by 2-fold while those of G233A, G234A, and F240A were decreased to approximately 50% of wild type. The reactivity of these mutants

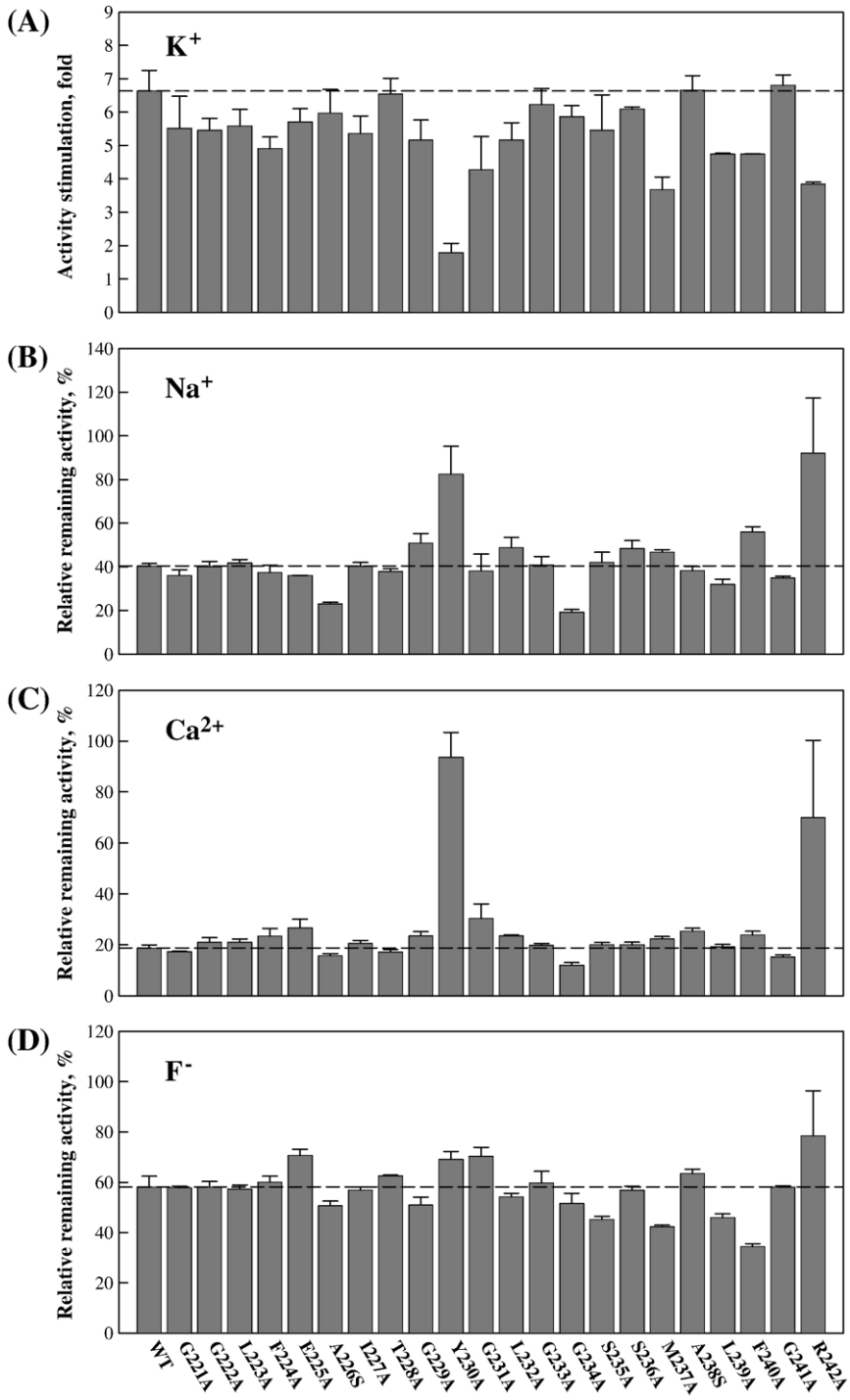

Fig. 4. Ion effects on mutant V-PPases. Microsomal membranes were prepared and enzymatic activities determined with various concentrations of ions as described under Materials and methods. The concentrations of ions were: 50 mM K^+, 100 mM Na^+, 0.1 mM Ca^{2+}, and 10 mM F^-, respectively. Values are means ± S.D. from at least 3 separate experiments.

depends obviously on the hydrolysis of PP_i, regardless the changes in K_M values of these mutants. In addition, two mutants of Group 1, L239A and F240A, displayed significant changes in optimal pH for PP_i hydrolysis (by approximately 0.5 pH units) and thermal stability of the enzyme (in more than 6 °C shift of $T_{1/2}$). It is conceivable that the apparent enzymatic activities of Group 1 among TM5 mutants were not considerably modified; albeit, they might presumably undergo several variations in their structure upon mutation, resulting in differences in many kinetic properties.

In contrast, Group 2 of TM5 mutants showed at least 2-fold decrease in enzymatic activities. Group 2 contains an alanine residue (A238), a marvelous GYG motif (G229, Y230,

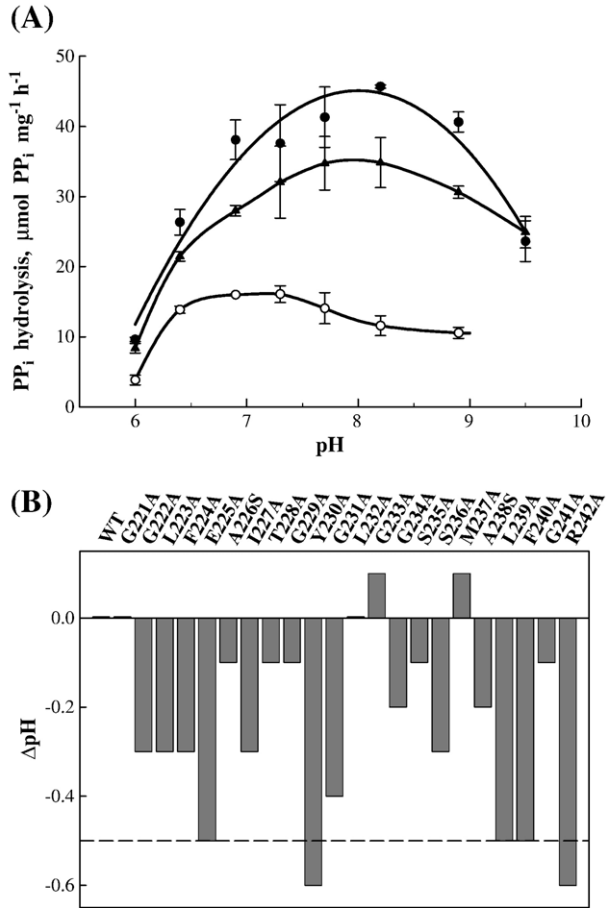

Fig. 5. Optimal pH for each mutant V-PPase. (A) The pH profile of enzymatic activities of several mutant V-PPases. PP_i hydrolysis of each mutant V-PPase was measured at different pH of reaction medium as described under Materials and methods. The pH values were maintained using 30 mM Tris–Mes. (●), WT; (○), E225A; (▲), M237A. Values are means ± S.D. from at least 3 separate experiments. (B) The shift of optimal pH of mutant V-PPases. Negative values indicate the shift toward acidic pH.

G231), and the only two charged residues (E225 and R242) along TM5. Substitution of charged residue R242 by alanine almost abolishes enzymatic and proton-translocating activities, while that of E225 brings both reactions to approximately 50% of wild type. Residue R242 was predicted to be located in the membrane–cytosol interface flanking N-terminal end of the putative substrate-binding loop (CL3). Likewise, E225 was proposed to reside in the lumen side of TM5. However, the possibilities of direct/or indirect involvement of these two charged residues in proton translocation, such as forming proton channel, are excluded since their apparent coupling ratios are not significantly changed. Furthermore, mutation of charged residues on TM5 decreased the heat tolerance of the V-PPase and shifted the optimal pH of enzymatic activities to be more acidic regardless their original charges. It is thus possible that these charged residues might play only a structural role, perhaps by stabilizing interactions between TM5 and adjacent transmembrane helices involved in proton translocation. Besides, replacement of R242 by alanine modifies the impacts of cations but not anion on the enzymatic activity, while that of E225 shows no considerable change in any ion effect. It is speculated that the R242 on the membrane–cytosol interface may directly or indirectly participate in the binding of cations, such as a salt-bridge, to V-PPase.

Moreover, mutations in the middle of the TM5 (G229 to G231 of Group 2) were more deleterious than other portions. These three residues (GYG motif) may presumably play a crucial role in sustaining the enzymatic reaction of vacuolar H^+-PPase. Furthermore, the apparent coupling ratios of mutants at this motif are decreased to below 50% of wild type, indicating that this motif might be directly or indirectly involved in the proton translocation. Replacement of residues in this motif by alanine decreased the heat tolerance of G229A and Y230A, but not G231A. Meanwhile, substitution of Y230 and G231 but not that of G229

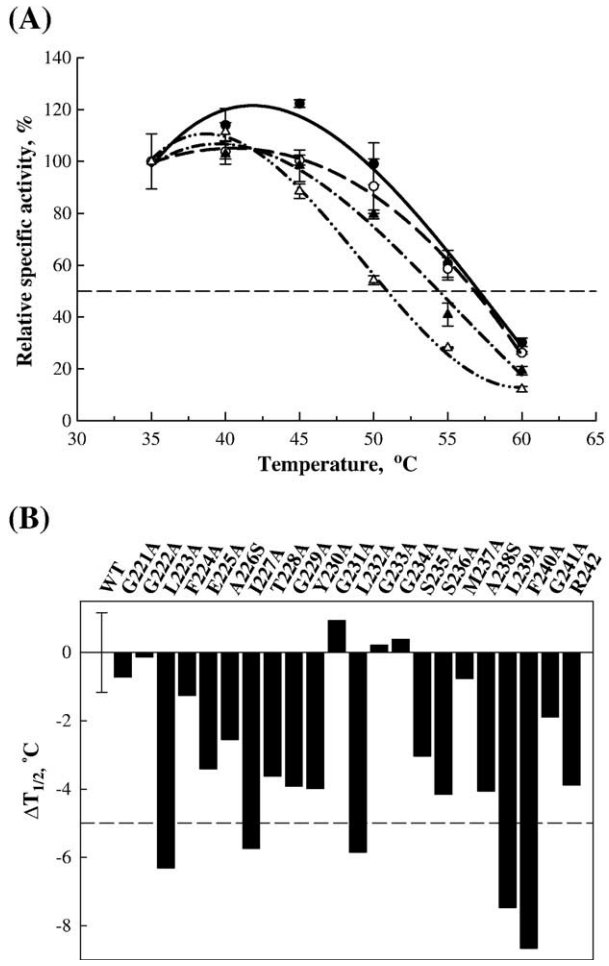

Fig. 6. Thermostability of mutant V-PPases. (A) Relative enzymatic activities of several mutant V-PPases at different temperature. Microsomal membrane fractions were routinely prepared and pre-treated at different temperature followed by cooling on ice bath. The enzymatic activities of heat-treated V-PPases were then measured and $T_{1/2}$ values determined as described under Materials and methods. Values are means ± S.D. from at least 3 separate experiments. (●), WT; (○), G222A; (▲), A238S; (△), L239A. (B) The shift of $T_{1/2}$ ($\Delta T_{1/2}$) for each mutant V-PPases. Negative values indicate the shift toward lower temperature.

of the motif by alanine shifted the pH optima of enzymatic activities by 0.4–0.5 units. The roles of these residues in maintaining the enzymatic reaction of the V-PPase may not be the same. However, further investigation indicates that the mutation at Y230 of GYG motif modifies the cation effects but not that of F^- inhibition. It is suggested that Y230 of the GYG motif may participate substantially in the cation binding of V-PPase. Moreover, recent biochemical and phylogenetic analysis identified A460 of H^+-PPase from *C. hydrogenoformans* (equivalent to A537 of mung bean V-PPase) as the K^+ binding site [8]. If this is the case, we speculate that the region containing GYG of TM5 may fold into the vicinity of the K^+ binding site of plant vacuolar H^+-PPase. Nevertheless, we could not exclude other alternatives, such as that GYG motif per se may form a cage for the K^+ binding, either on individual subunits or at the dimeric interface of plant V-PPase. Furthermore, a line of evidence reveals that several K^+-selective channel subfamilies from bacteria, plants, and animals contain a highly conserved GYG motif as a signature pore sequence [27–31]. It is thus suggested that GYG motif is the intrinsic property of pore architecture for K^+ selectivity over Na^+ in ion channels [30]. Our current work demonstrated the relief of cation effects upon mutation of GYG motif, implicating its possible involvement in cation binding in mung bean V-PPase. It is noteworthy to further elucidate potential role(s) and exact structure of this novel motif in proton-translocating PPase of higher plants.

Acknowledgements

This work was supported by the grant from National Science Council, Republic of China (NSC 93-2311-B-007-003) to RLP. We sincerely appreciate Mr. Oscar Ting for his critical reading of the manuscript.

References

[1] M. Maeshima, Vacuolar H^+-pyrophosphatase, Biochim. Biophys. Acta 1465 (2000) 37–51.
[2] M. Maeshima, Tonoplast transporters: organization and function, Annu. Rev. Plant Physiol. Plant Mol. Biol. 52 (2001) 469–497.
[3] C.M. Tzeng, C.Y. Yang, S.J. Yang, S.S. Jiang, S.Y. Kuo, S.S. Hung, J.T. Ma, R.L. Pan, Subunit structure of vacuolar proton-pyrophosphatase as determined by radiation inactivation, Biochem. J. 316 (1996) 143–147.
[4] R. Gordon-Weeks, S.H. Steele, R.A. Leigh, The role of magnesium, pyrophosphate, and their complexes as substrates and activators of the vacuolar H^+-pumping inorganic pyrophosphatase, Plant Physiol. 111 (1996) 195–202.
[5] R.R. Walker, R.A. Leigh, Mg^{2+}-dependent, cation-stimulated inorganic pyrophosphatase associated with vacuoles isolated from storage roots of red beet (*Beta vulgaris* L.), Planta 153 (1981) 150–155.
[6] M. Maeshima, H^+-translocating inorganic pyrophosphatase of plant vacuoles: inhibition by Ca^{2+}, stabilization by Mg^{2+} and immunological comparison with other inorganic pyrophosphatases, Eur. J. Biochem. 196 (1991) 11–17.
[7] A.A. Baykov, E.B. Dubnova, N.P. Bakuleva, O.A. Evtushenko, R.-G. Zhen, P.A. Rea, Differential sensitivity of membrane-associated pyrophosphatases to inhibition by diphosphonates and fluoride delineates two classes of enzyme, FEBS Lett. 327 (1993) 199–202.
[8] G.A. Belogurov, R.A. Lahti, A lysine substitute for K^+: A460K mutation eliminates K^+ dependence in H^+-pyrophosphatase of *Carboxydothermus hydrogenoformans*, J. Biol. Chem. 277 (2002) 49651–49654.
[9] Y.M. Drozdowicz, P.A. Rea, Vacuolar H^+ pyrophosphatases: from the evolutionary backwaters into the mainstream, Trends Plant Sci. 6 (2001) 206–211.
[10] M.T. McIntosh, A.B. Vaidya, Vacuolar type H^+ pumping pyrophosphatases of parasitic protozoa, Int. J. Parasitol. 32 (2002) 1–14.
[11] A. Takasu, Y. Nakanishi, T. Yamanuchi, M. Maeshima, Analysis of the substrate binding site and carboxyl terminal region of vacuolar H^+-pyrophosphatase of mung bean with peptide antibodies, J. Biochem. (Tokyo) 122 (1997) 883–889.
[12] E.J. Kim, R.-G. Zhen, P.A. Rea, Site-directed mutagenesis of vacuolar H^+-pyrophosphatase: necessity of Cys^{634} for inhibition by maleimides but not catalysis, J. Biol. Chem. 270 (1995) 2630–2635.
[13] R.-G. Zhen, E.J. Kim, P.A. Rea, Acidic residues necessary for pyrophosphate-energized pumping and inhibition of the vacuolar H^+-pyrophosphatase by *N,N′*-Dicyclo-hexylcarbodiimide, J. Biol. Chem. 272 (1997) 22340–22348.
[14] S.J. Yang, S.S. Jiang, S.Y. Kuo, S.H. Hung, M.F. Tam, R.L. Pan, Localization of a carboxylic residue possibly involved in the inhibition of vacuolar H^+-pyrophosphatase by *N,N′*-dicyclohexylcarbodiimide, Biochem. J. 342 (1999) 641–646.
[15] Y. Nakanishi, T. Saijo, Y. Wada, M. Maeshima, Mutagenic analysis of functional residues in putative substrate binding site and acidic domains of vacuolar H^+-pyrophosphatase, J. Biol. Chem. 276 (2001) 7654–7660.
[16] M.G. Claros, G. von Heijne, TopPreda II: An improved software for membrane protein structure predictions, Comput. Appl. Biosci. 10 (1994) 685–686.
[17] R.D. Gietz, R.H. Schiestl, A.R. Willems, R.A. Woods, Studies on the transformation of intact yeast cells by the LiAc/SS-DNA/PEG procedure, Yeast 11 (1995) 355–360.
[18] S. Barik, Site-directed mutagenesis by double polymerase chain reaction: megaprimer method, in: B.A. White (Ed.), Methods Mol. Biol., vol. 15, Humana, New Jersey, 1993, pp. 277–286.
[19] Y.Y. Hsiao, R.C. Van, S.H. Hung, H.H. Lin, R.L. Pan, Roles of histidine residues in plant vacuolar H^+-pyrophosphatase, Biochim. Biophys. Acta 1608 (2004) 190–199.
[20] C.H. Fiske, Y. Subbarow, The colorimetric determination of phosphorus, J. Biol. Chem. 66 (1925) 375–400.
[21] M.Y. Wang, Y.H. Lin, W.M. Chow, T.P. Chung, R.L. Pan, Purification and characterization of tonoplast ATPase from etiolated mung bean seedlings, Plant Physiol. 90 (1989) 475–481.
[22] M. Bradford, A rapid and sensitive method for the quantitation of microgram quantities of protein utilizing the principle of protein-dye binding, Anal. Biochem. 72 (1976) 248–254.
[23] P.A. Rea, J.C. Turner, Tonoplast adenosine triphosphatase and inorganic pyrophosphatase, in: P.J. Lea (Ed.), Methods Plant Biochem., vol. 3, Academic Press, London, 1990, pp. 385–405.
[24] H. Rottenberg, The measurement of membrane potential and delta pH in cells, organelles, and vesicles, in: S. Fleischer, L. Packer (Eds.), Methods Enzymol., vol. 55, Academic Press, New York, 1979, pp. 547–569.
[25] S. Clerc, Y. Barenholz, A quantitative model for using acridine orange as a transmembrane pH gradient probe, Anal. Biochem. 259 (1998) 104–111.
[26] U.K. Laemmli, Cleavage of structural proteins during the assembly of the head of bacteriophage T4, Nature 222 (1970) 680–685.
[27] D.A. Doyle, J.M. Cabral, R.A. Pfuetzner, A. Kuo, J.M. Gulbis, S.L. Cohen, B.T. Chait, R. MacKinnon, The structure of the potassium

channel: molecular basis of K^+ conduction and selectivity, Science 280 (1998) 69–76.
[28] C. Miller, See potassium run, Nature 414 (2001) 23–24.
[29] J.H. Morais-Cabral, Y. Zhou, R. MacKinnon, Energetic optimization of ion conduction rate by the K^+ selectivity filter, Nature 414 (2001) 37–42.
[30] Y. Jiang, A. Lee, J. Chen, M. Cadene, B.T. Chait, R. MacKinnon, Crystal structure and mechanism of a calcium-gated potassium channel, Nature 417 (2002) 515–522.
[31] B.-G. Hua, R.W. Mercier, Q. Leng, G.A. Berkowitz, Plants do it differently. A new basis for potassium/sodium selectivity in the pore of an ion channel, Plant Physiol. 132 (2003) 1353–1361.